Journal of Solid State Chemistry 183 (2010) 1102–1107

Contents lists available at ScienceDirect

Journal of Solid State Chemistry

journal homepage: www.elsevier.com/locate/jssc

R-site varied series of $RBaCo_2O_{5.5}$ ($R_2Ba_2Co_4O_{11}$) compounds with precisely controlled oxygen content

Eeva-Leena Rautama, Maarit Karppinen *

Laboratory of Inorganic Chemistry, Department of Chemistry, Aalto University School of Science and Technology, P.O. Box 16100, FI-00076, Aalto, Finland

ARTICLE INFO

Article history:
Received 16 November 2009
Received in revised form
4 March 2010
Accepted 7 March 2010
Available online 15 March 2010

Keywords:
Double perovskite
Cation ordering
Oxygen stoichiometry
Chemical pressure

ABSTRACT

The entire family of carefully oxygen-adjusted $RBaCo_2O_{5.5}$ or $R_2Ba_2Co_4O_{11}$ (R=Y, Ho–La) double-perovskite oxides is systematically investigated for the lattice parameters, *A*-site cation disorder, and characteristic physical properties, i.e. the metal–insulator transition, ferromagnetic transition and so-called metamagnetic transition. With increasing size of the *R* constituent, the lattice parameters start to deviate from the linear behavior, indicating partial oxygen/vacancy and *A*-site cation disorder for the largest *R*s of Nd, Pr and La. Both the metal–insulator transition and the two magnetic transitions are found to be highly sensitive to even minor deviations from the ideal 5.5 oxygen stoichiometry, thus underlining the importance of proper oxygen-content adjustment.

1. Introduction

The oxygen-deficient *A*-site ordered double-perovskite structure was first realized for $RBa(Cu_{0.5}Fe_{0.5})_2O_{5+\delta}$ with R=Y in 1988 [1]. Later the same structure has been revealed for compounds with various *R* and *B* site constituents. The cobalt-based system, $RBaCo_2O_{5+\delta}$ (R=Y, Ho–La) [2,3], in particular has been the target of intensive studies after the discoveries of phenomena such as relatively large magnetoresistance effect [4] and metal–insulator transition [5,6] for $RBaCo_2O_{5+\delta}$ samples with the oxygen content at δ=0.5 or in the vicinity of it.

The $RBaCo_2O_{5+\delta}$ structure is composed of [CoO_2] layers separated by alternate layers of [BaO] and [RO_δ] to double the perovskite cell along the *c* axis. At δ=0.5, also the oxygen atoms and vacancies within the RO_δ layer are ordered, creating alternating octahedral and pyramidal coordination polyhedra for the trivalent Co ions. As a result, the perovskite unit cell is also doubled along the *b* direction [7]. This is illustrated in Fig. 1.

The ideal *A*-site-cation and oxygen/vacancy ordered $RBaCo_2O_{5.5}$ (or $R_2Ba_2Co_4O_{11}$) phase is somewhat difficult to realize except for the smallest *R* constituents (Y, Ho, Dy). Firstly, the stacking sequence of the [$RO_{0.5}$] and [BaO] layers gets readily irregular for the largest *R*s with the ionic radii close to that of divalent barium. Moreover, under ordinary conditions used for sample synthesis samples with $\delta > 0.5$ and lattice parameters and physical properties different from those at δ=0.5 are obtained for the intermediate-sized *R*s (Tb − Sm) and especially for the largest *R*s (Nd, Pr, La) for which even structural changes are seen upon oxygen-content deviation from the half occupancy.

The metastability of the $RBaCo_2O_{5.5}$ structure makes it readily absorb and desorb oxygen which can lead to both oxygen/vacancy disorder and substructures [3,8]. Hence it is crucially important to both control and determine the actual oxygen content precisely. There are several options for the precise oxygen-content determination, i.e. thermogravimetric (TG) reduction, wet-chemical redox titrations and neutron diffraction (ND). Even though a sensitive thermobalance may be accurate enough for detecting tiny mass changes, reductive decomposition to binary oxides and/or metals has proven not to be the best method for rare-earth cobaltites [9,10]. There are several issues that should be considered. One is the sensitivity of R_2O_3 oxides (especially with the large *R*s) to absorb humidity, another is the tendency for some of the *R*s to form not so well defined (mixed-valent) oxides and/or their mixtures (e.g. Pr_2O_3–Pr_6O_{11}–PrO_2, Tb_4O_7–Tb_6O_{11}, EuO–Eu_2O_3). Since ND is not always available, wet-chemical redox methods in which cobalt is reduced to its divalent state are very practical and accurate for oxygen-content determination. Both iodometric and cerimetric titration techniques can be used [9]. In the latter case the unavoidable precipitation of $BaSO_4$ may be considered harmful, and for this reason, iodometry should be preferred.

Owing to the apparent difficulties in both sample synthesis and proper oxygen-content adjustment and analysis, literature data for the various samples meant to represent the $RBaCo_2O_{5.5}$ system are somewhat scattered. Moreover, until now no systematic studies involving the complete series of $RBaCo_2O_{5.5}$

* Corresponding author. Fax: +358 9 462 373.
E-mail address: maarit.karppinen@tkk.fi (M. Karppinen).

0022-4596/$ - see front matter © 2010 Elsevier Inc. All rights reserved.
doi:10.1016/j.jssc.2010.03.011

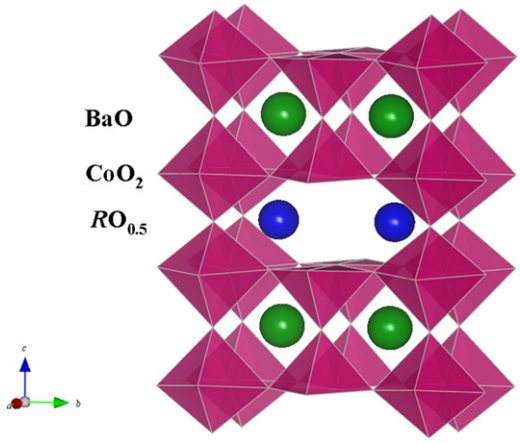

Fig. 1. Schematic crystal structure of RBaCo$_2$O$_{5.5}$ compounds with a 122-type ($a_p \times 2a_p \times 2a_p$) unit cell.

compounds with the "5.5" stoichiometry have been reported. Here we have synthesized high-quality samples of the RBaCo$_2$O$_{5+\delta}$ system with R=Y, Ho, Dy, Tb, Gd, Eu, Sm, Nd, Pr and La, carefully adjusted their oxygen contents to the target δ=0.5 value and characterized the oxygen-tuned samples for the evolution of the lattice parameters and A-site cation disorder as well as the metal–insulator and magnetic transition temperatures regarding the size of the R constituent or so-called chemical-pressure effect.

2. Experimental

Polycrystalline samples of RBaCo$_2$O$_{5+\delta}$ with R=Y, Ho, Dy, Tb, Gd, Eu, Sm, Nd and Pr were prepared through standard solid-state synthesis routes from stoichiometric amounts of pre-calcined R_2O_3 (except Pr_6O_{11} and Tb_4O_7), $BaCO_3$ and Co_3O_4 powders. All the samples were first calcined in air at 900 °C for 12 h, then pelletized and sintered at temperatures between 1100 and 1150 °C as long as it was needed to obtain a phase-pure sample and then slowly furnace-cooled down to room temperature. In practice, the synthesis time required varied from 36 to 120 h, increasing with decreasing ionic radius, $r(R^{3+})$. Samples with the smallest Rs (Y, Ho, Dy) were sintered in O_2 gas flow, others (except the R=La sample) in air. The data for the LaBaCo$_2$O$_{5.5}$ compound are from Ref. [3] where its synthesis is described in detail. In brief, the material was synthesized from a sol–gel-based precursor under Ar gas (5 N) flow at 1150 °C for 48 h, then oxygenated under pressurized O_2 (100 bar) and treated at 590 °C in Ar flow for 12 h to reach the target 5.5 oxygen-content value.

Phase purity of the as-synthesized samples was confirmed with a laboratory X-ray powder diffractometer (XRD; PanAnalytical X'Pert PRO MPD, Cu$K\alpha$1 radiation) at room temperature in the 2θ range 10°–100°. Oxygen content was determined (by means of iodometry) for each sample to guide the subsequent oxygen-adjustment annealings. These annealings were carried out either in a thermobalance (Perkin Elmer Pyris 1 TGA) or in a tight tube furnace at pre-selected temperatures under Ar gas (5 N) flow of 100 ml/min. In the former/latter case, the sample amount was ca. 100 mg/1 g. Heating and cooling rates were kept slow (2 °C/min) to enable better cation and oxygen/vacancy ordering within the materials. The samples were kept at the annealing temperature for 3 h.

Iodometric titrations were carried out not only for the as-synthesized samples but also for all the oxygen-adjusted samples. About 30 mg of the finely ground sample powder was dissolved in 1 M HCl (bubbled thoroughly from dissolved oxygen) together with an excess of potassium iodide (ca. 1.5 g) in an air-tight cell under constant N_2 (5 N) bubbling. The thus formed iodine was then titrated with standard 0.100 M $Na_2S_2O_3$ solution (Merck) in the presence of starch indicator, added close to the end point. Each experiment was repeated three to four times with excellent reproducibility (less than $\pm$0.005 variation for δ).

The final oxygen-adjusted samples were characterized for the lattice parameters, determined from the XRD patterns using the Rietveld refinement program FullProf [11]. Differential scanning calorimetry (DSC; Perkin Elmer Diamond) measurements were carried out to probe the metal–insulator transition reported for several RBaCo$_2$O$_{5.5}$ compounds above room temperature [5–7]. The measurements were performed within the temperature range of 300–400 K using sealed aluminum pans. Heating and cooling rates were 20 °C/min and N_2 was used as a protective and purging gas. Magnetization (M) was measured for the samples in zero-field-cooled (ZFC) and field-cooled (FC) modes with a SQUID magnetometer (MPMS-XL, Quantum Design) between 5 and 400 K under an applied field of 0.1 T.

3. Results and discussion

Oxygen-content adjustment: The as-air-synthesized, furnace-cooled RBaCo$_2$O$_{5+\delta}$ samples with R=Gd, Eu, Sm, Nd and Pr were oxygen-rich with $\delta > 0.50$ as expected, and these samples were oxygen-depleted in Ar gas flow at appropriate temperatures. Relatively good estimates for the proper annealing temperatures were obtained from the pre-information gathered from TG measurements. Nevertheless, several heat treatments were often required at gradually increased temperatures to reach the target oxygen-content value of 5.50 as precisely as possible. For the R=Y, Ho, Dy and Tb samples, either synthesis or post-annealing in O_2 gas flow was required to obtain the 5.5 stoichiometry. Moreover, in the case of TbBaCo$_2$O$_{5+\delta}$, it was noticed that upon treating the sample in O_2 flow, the oxygen content increased from the value of δ=0.398 for the as-air-synthesized sample to δ=0.556, the latter being too far from the target. To avoid additional back-reduction, low-temperature oxygenation in air at 320 °C for 12 h was employed instead. This resulted in an acceptable δ value of 0.514. Oxygen contents for the as-air-synthesized samples, conditions used for the oxygen-adjustment and the final oxygen contents of the "5.5 samples" are gathered in Table 1. Moreover, in Fig. 2 we plot the δ values of the as-air-synthesized samples to illustrate the dependence on $r(R^{3+})$. Finally we should mention that in the case of the R=La member, the as-Ar-synthesized LaBaCo$_2$O$_{5+\delta}$ sample was first oxygenated up to $\delta \approx 1$ under pressurized oxygen (100 bar) and

Table 1
Oxygen stoichiometry parameter δ of the as-air-synthesized RBaCo$_2$O$_{5+\delta}$ samples together with the final annealing conditions and oxygen contents of the oxygen-adjusted "5.5 samples". The values in parenthesis are standard deviations.

R^{3+}	δ (as-synth.)	Ann. cond.	δ (adjusted)
La[a]	–	–	0.52(1)
Pr	0.777(5)	790 °C, Ar, 3 h	0.501(6)
Nd	0.702(5)	570 °C, Ar, 3 h	0.512(7)
Sm	0.599(5)	360 °C, Ar, 3 h	0.492(5)
Eu	0.552(4)	310 °C, Ar, 3 h	0.499(5)
Gd	0.515(2)	260 °C, Ar, 3 h	0.502(4)
Tb	0.398(4)	330 °C, air, 12 h	0.514(5)
Dy	–	Synth. in O_2	0.492(5)
Ho	–	Synth. in O_2	0.511(5)
Y	–	Synth. in O_2	0.495(5)

[a] Data taken from Ref. [3].

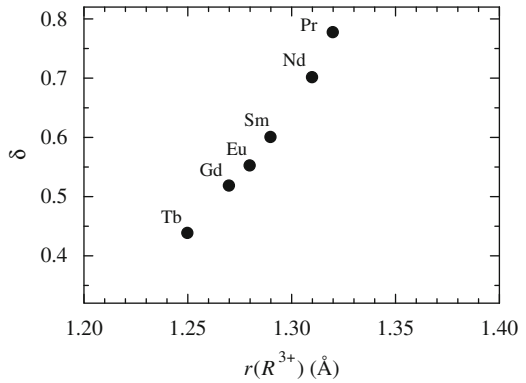

Fig. 2. Oxygen non-stoichiometry parameter δ of the as-air-synthesized RBaCo$_2$O$_{5+\delta}$ samples plotted against the ionic radius of the R constituent, $r(R^{3+})$.

Table 2
Lattice parameters and unit-cell volume for oxygen-adjusted RBaCo$_2$O$_{5.5}$ samples. The fractional occupancy factor, $g(R^{3+})$, is also given for selected samples.

R^{3+}	a (Å)	$b/2$ (Å)	$c/2$ (Å)	V (Å^3)	g (R^{3+})
Y[a]	3.8482(2)	3.9094(2)	3.7511(2)	56.43(1)	
Ho	3.8527(1)	3.9090(1)	3.7556(1)	56.57(1)	
Dy	3.8594(3)	3.9101(1)	3.7555(1)	56.67(1)	
Tb	3.8701(1)	3.9102(1)	3.7595(1)	56.89(1)	0.996(2)
Gd	3.8779(2)	3.9163(2)	3.7668(2)	57.20(1)	–
Eu	3.8838(1)	3.9206(1)	3.7709(1)	57.34(1)	–
Sm	3.8879(2)	3.9237(1)	3.7774(1)	57.62(1)	0.991(2)
Nd	3.9011(1)	3.9336(2)	3.7959(2)	58.25(1)	0.944(2)
Pr	3.9076(1)	3.9365(1)	3.8056(1)	58.54(1)	0.908(3)
La[b]	3.9264(4)	3.9605(2)	3.8485(2)	59.84(1)	

[a] Phase abundance 90.9(1)%.
[b] Data taken from Ref. [3].

then treated at 590 °C for 12 h under Ar flow to obtain the 5.5 phase [3].

Lattice behavior: Starting points for the structural models were taken from Refs. [8,12–21]. For all the 5.5 compounds a "122-type" unit cell of $a_p \times 2a_p \times 2a_p$ with space group *Pmmm* was assumed. The main purpose of the refinements was to obtain the lattice parameters for comparison within the RBaCo$_2$O$_{5.5}$ series. Yet, the degree of *A*-site cation order was additionally studied and therefore the Rietveld method was employed instead of just Le Bail profile fitting. It is worth to mention that some of the small members have been found to crystallize in a $2a_p \times 2a_p \times 2a_p$ structure with space group *Pmma* [19,21–23]. This was tested here too and found not to have any significant effect on the lattice parameters, thereby justifying the choice of the 122 structure for the present work. All the refinements were conducted assuming a perfect RBaCo$_2$O$_{5.5}$ structure, meaning no additional (or lacking) oxygen was taken into account.

Table 2 lists the refined structural parameters. Lattice parameters together with the unit-cell volume V are moreover plotted in Fig. 3 as a base for the following discussion (full circles). Literature data for various RBaCo$_2$O$_{5+\delta}$ samples (assigned by the authors to represent the "5.5 phases") are also included in Fig. 3 (hollow circles). Before further discussions it should be mentioned that we also characterized some off-stoichiometric samples to reveal that an increase in the oxygen content causes b parameter to decrease and c parameter to increase. From Fig. 3, a continuous increase in lattice parameter a with increasing $r(R^{3+})$ is verified for the $\delta = 0.5$ samples. Apparently the a parameter is not affected by small variations in oxygen content possibly existing within the samples (present+literature) included in Fig. 3, whereas there is much more scattering seen for the parameter b. Among the present samples (filled circles), only the R=Tb sample is vaguely out of the trend, which is consistent with the slightly over-stoichiometric oxygen content that makes the lattice contract along the b axis. For parameter c (and also for the unit-cell volume V) a linear increase with increasing $r(R^{3+})$ is seen for the samples with small and medium-sized rare earth constituents whereas those with R=(Sm), Nd, Pr and La somewhat deviate from the linear behavior. This is attributed to a gradually lowered degree of order within the *A*-cation sublattice. The change in the slope of parameter b (about R=Eu) is tentatively attributed to increasing oxygen/vacancy disorder with increasing $r(R^{3+})$. Note that the doubling of the b parameter in the 122 unit cell originates from the oxygen/vacancy ordering. Recent reports have underlined the tendency of the PrBaCo$_2$O$_{5.5}$ and LaBaCo$_2$O$_{5.5}$ compounds to exhibit partial (~10%) oxygen/vacancy disorder [3,8,24]. In Refs. [8,24], an improved synthesis route to obtain highly oxygen/vacancy ordered PrBaCo$_2$O$_{5.5}$ is described. Unfortunately, the authors do not present the lattice parameters for their highly ordered PrBaCo$_2$O$_{5.5}$ sample, and hence we are not able to see where the R=Pr datum point would place in Fig. 3 without the disorder effect.

The degree of *A*-site cation order was investigated for representative *R*s by refining the fractional occupancies of *R* and Ba atoms at the two *A*-cation sites. The results indeed revealed—within the limits of XRD—a certain level of disorder for our R=Nd and Pr samples, whereas e.g. for the R=Tb sample the results indicated essentially perfect ordering (see Table 2).

To play little further with the lattice parameter data, we show in Fig. 4 the c versus $r(R^{3+})$ plot for the as-air-synthesized R=Tb, Gd, Eu, Sm, Nd and Pr samples. For the same samples the δ versus $r(R^{3+})$ plot was shown in Fig. 2, revealing essentially linear behavior from R=Tb up to Pr. Now for the c parameter the linear dependency extends only up to R=Sm, indicating cation disorder for the R=Nd and Pr samples. Hence we conclude that the *A*-site cation disorder is not induced by the reductive annealing but exists already in the as-air-synthesized R=Nd and Pr samples.

Metal–insulator transition: Differential scanning calorimetry was used to investigate the effects of oxygen off-stoichiometry and chemical pressure on the metal–insulator transition seen for the RBaCo$_2$O$_{5.5}$ compounds above room temperature. As has been shown earlier, the metal–insulator transition is accompanied by a strong, reversible calorimetric effect [25,26]. Fig. 5 presents DSC heating scans for TbBaCo$_2$O$_{5+\delta}$ with different oxygen contents. The effect of oxygen off-stoichiometry is prominent. Clearly seen is an increase in the enthalpy when getting closer to the 5.5 stoichiometry, accompanied by a change in the transition temperature T_{M-I}. The chemical-pressure effect on the DSC heating scans is depicted in Fig. 6 and the inset shows the T_{M-I} values (determined from the scans). The R=Y and Ho samples did not present any calorimetric effect in the present temperature measurement range, as the T_{M-I} values of these two samples probably fall below 300 K [25]. The mass-corrected enthalpy turned out to be very similar for the oxygen-adjusted R=Tb–Sm samples (Fig. 6) but significantly smaller for the corresponding oxygen off-stoichiometric samples (Fig. 5). It moreover seems that also the oxygen/vacancy disorder might have an effect on the magnitude of enthalpy [27]. This was evidenced in the case of the PrBaCo$_2$O$_{5.5}$ phase, for which we employed various lengths of the post-synthesis Ar annealing: the longer annealing somewhat increased the magnitude of enthalpy (not shown here). On the other hand, from Fig. 6 clearly seen is that DSC peak gets broader/weaker for the large *R*s. We calculated the FWHM values of the enthalpy change which gave 3.9(2) K for R=Pr and Nd, 2.8(2) K for R=Sm and 1.5(2)–2.1(2) K for R=Dy–Eu. It is reasonable to assume that the peak broadening/weakening is due to the disorder effect. If there is only 80–90% of the properly ordered phase present, it is rather natural to observe a weaker peak.

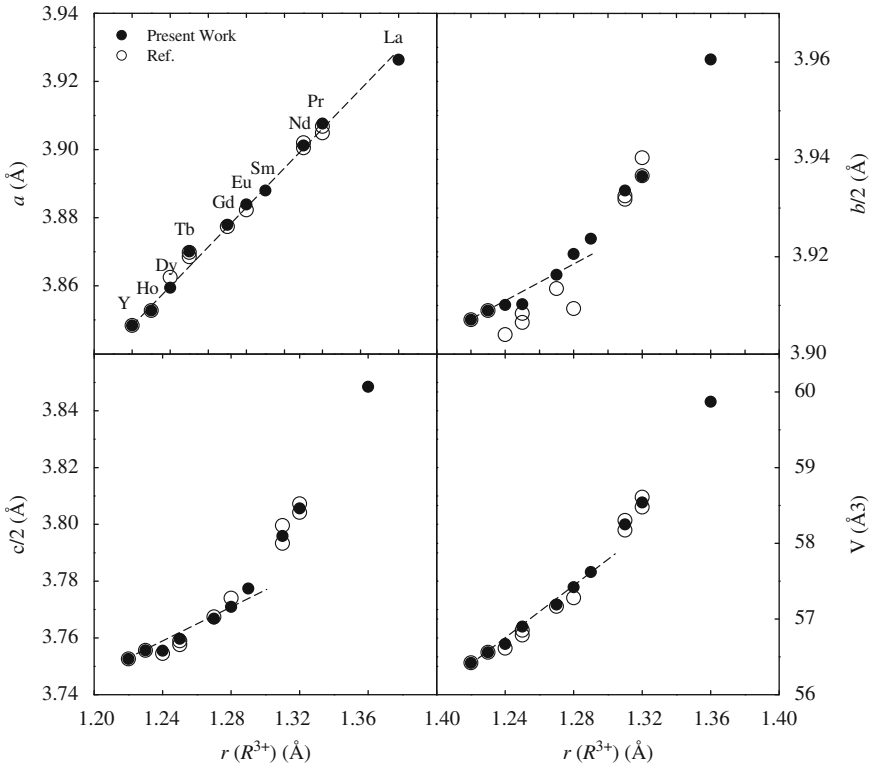

Fig. 3. Evolution of the lattice parameters, *a*, *b* and *c*, and unit-cell volume, *V*, for $RBaCo_2O_{5.5}$ samples: filled circles for this work and hollow circles for literature data [8,12–21]. The lines are guides for the eye.

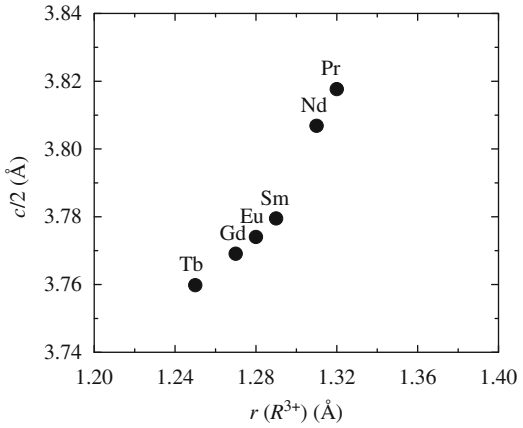

Fig. 4. Evolution of the lattice parameter *c* for as-air-synthesized $RBaCo_2O_{5+\delta}$ samples plotted against the ionic radius of the *R* constituent, $r(R^{3+})$.

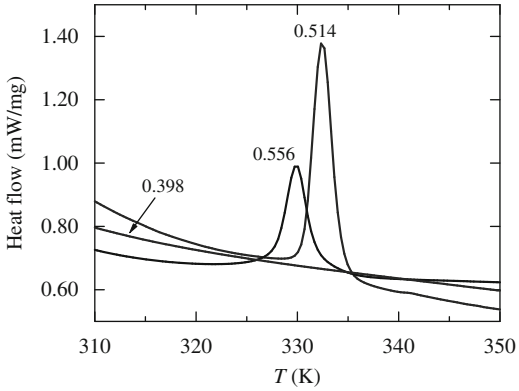

Fig. 5. DSC heating scans recorded with a heating rate of 20 °C/min for $TbBaCo_2O_{5+\delta}$ samples with various δ-values.

Regarding the transition temperatures in the inset of Fig. 6, it should first be mentioned that the absolute values of T_{M-I} may deviate from one study to another as it depends on the heating rate employed. In the present work the relatively fast heating rate (20 °C/min) used shifts the T_{M-I} values to the higher temperatures. From Fig. 6, T_{M-I} first increases along $r(R^{3+})$ but then starting from R=Nd drops significantly for the largest *R*s.

Magnetic properties: Fig. 7(a) presents the magnetization versus temperature curves for the oxygen-adjusted $RBaCo_2O_{5.5}$ samples (For R=La, see Ref. [3]). The materials exhibit magnetic behavior typical of this family [5–7], that is, a spontaneous magnetization which then turns to antiferromagnetic ordering at lower temperatures. In the oxygen-adjusted samples, the ZFC and FC curves converge and overlap fully, lacking any sign of secondary ordering after the antiferromagnetic transition, which is not always clear from earlier data for "5.5 phases". The first magnetic transition occurs in a narrow temperature range at temperatures somewhat below room temperature, the transition temperature T_C (determined from the dM/dT curves) depending on the particular R such that with decreasing $r(R^{3+})$ T_C increases except for the end members, R=La and Y, see Fig. 7(b). In Fig. 7(b) we also plot the so-called metamagnetic transition temperature T_m [19] for the same samples that represents the maximum in magnetic susceptibility. Nearly similar trend in terms of $r(R^{3+})$ is seen for T_m compared to that for T_C. The unusual shape of the R=Y magnetization curve is explained by co-existence of two phases. We could fit our XRD data in a satisfactory manner (χ^2=3.07, R_{Bragg}=10.3%) assuming the δ=0.44 phase with a "332-type" *P*4/*nmm* structure [21] as the secondary phase; the fitting yielded an abundance of 9.07(6)% for this phase. Quite interestingly, the existence of the δ=0.44 minority phase with 9% abundance yields an average oxygen content for the sample at 5.495 which is

exactly the value obtained from iodometric titration. Here we should also mention that the magnetization of the $\delta=0.44$ phase is stronger than that of the $\delta=0.50$ phase [25,28].

As for the effect of oxygen off-stoichiometry, in overall we noticed that the temperature range of the spontaneous magnetization gets narrower by 10–20 K in the oxygen-adjusted samples compared to the corresponding off-stoichiometric materials, as illustrated in Fig. 7(c) in the case of R=Tb. The present oxygen-adjusted $TbBaCo_2O_{5.51}$ sample lacks the secondary magnetic transition observed near 170 K by previous workers [16,29]. In a close examination of the magnetization data for our oxygen over-stoichiometric $TbBaCo_2O_{5.56}$ sample, the inverse susceptibility, χ^{-1}, reveals a hump at ~175 K (not shown here), suggesting that the lower-temperature secondary magnetic transition is related to the oxygen off-stoichiometry.

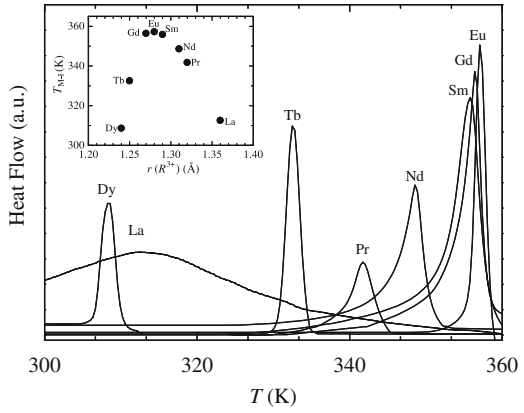

Fig. 6. DSC heating scans recorded with a heating rate of 20 °C/min for oxygen-adjusted $RBaCo_2O_{5.5}$ samples. The inset shows the metal–insulator transition temperatures T_{M-I} plotted against the ionic radius of the R constituent, $r(R^{3+})$.

For the present oxygen-adjusted samples, with increasing $r(R^{3+})$ the ZFC and FC curves start to separate for R=Sm. According to the previous reports for the R=Pr member [8,12], magnetic susceptibility is affected by the partial oxygen/vacancy disorder. The disorder results in a large separation between the ZFC and FC curves, as noticed here too. The separation has been shown to vanish for R=Pr when the oxygen/vacancy ordering is enhanced [24]. The oxygen/vacancy disorder is most likely behind the ZFC–FC separation also in the case of the $NdBaCo_2O_{5.5}$ sample. Note that the lattice parameters indicated partial disorder for this material too. Even though there are several reports that deal with $NdBaCo_2O_{5.5}$, only in Ref. [30] is the FC magnetization shown, thus comparison is difficult. Surprisingly, for $LaBaCo_2O_{5.52}$ the $M(T)$ curve does not resemble the behavior measured for the R=Pr and Nd samples even though neutron diffraction and high-resolution transmission electron microscopy data indicated similar oxygen/vacancy disorder [3]. The La-based compound [3,31] rather resembles $SmBaCo_2O_{5.5}$ except for the abnormal transition temperature.

4. Conclusions

We have systematically investigated the $RBaCo_2O_{5.5}$ family of A-site-cation and oxygen ordered double-perovskite oxides for their basic (crystal) chemical and physical properties in terms of the size of the R constituent. Our study comprises all the existing members of the family (i.e. R=Y, Ho, Dy, Tb, Gd, Eu, Sm, Nd, Pr and

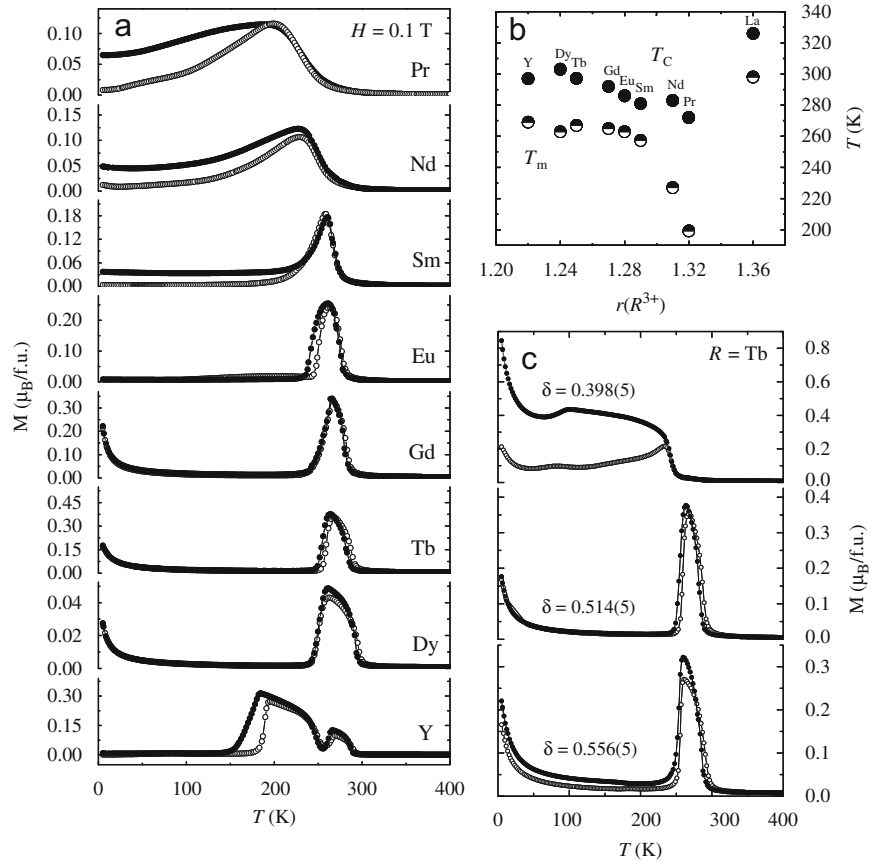

Fig. 7. (a) ZFC (hollow circles) and FC (filled circles) magnetization of oxygen-adjusted $RBaCo_2O_{5.5}$ samples measured under 0.1 T and (b) their Curie (T_C, full circles) and metamagnetic (T_m, half filled circles) transition temperatures. (c) Magnetization of $TbBaCo_2O_{5+\delta}$ samples with various oxygen contents. The data for R=La is taken from Ref. [3].

La) and involves samples with the oxygen content carefully adjusted to the ideal 5.5 value. The results strongly underline the sensitivity of both the crystal features and physical properties to even tiny deviations of oxygen content from the target value. Moreover, not only the overall oxygen stoichiometry but also the distribution of oxygen/oxygen vacancies play a role as also does the stacking disorder among the [$RO_{0.5}$] and [BaO] layers. Our study has clearly demonstrated that the disorder effects get enhanced with increasing $r(R^{3+})$ becoming prominent for samples with the three largest R constituents of Nd, Pr and La.

Acknowledgments

This work was supported by Academy of Finland (no. 126528). The authors thank Prof. Vincent Caignaert, Prof. Bernard Raveau, Dr. Valérie Pralong and Prof. Hisao Yamauchi for discussions. E.-L. Rautama acknowledges financial support from the Finnish Foundation for Technology Promotion.

References

[1] L. Er-Rakho, C. Michel, Ph. Lacorre, B. Raveau, J. Solid State Chem. 73 (1988) 531.
[2] W. Zhou, C.T. Lin, W.Y. Liang, Adv. Mater. 5 (1993) 735;
W. Zhou, Chem. Mater. 6 (1994) 441.
[3] E.-L. Rautama, V. Caignaert, Ph. Boullay, A.K. Kundu, V. Pralong, M. Karppinen, C. Ritter, B. Raveau, Chem. Mater. 21 (2009) 102.
[4] C. Martin, A. Maignan, D. Pelloquin, N. Nguyen, B. Raveau, Appl. Phys. Lett. 71 (1997) 1421.
[5] I.O. Troyanchuk, N.V. Kasper, D.D. Khalyavin, Phys. Rev. Lett. 80 (1998) 3380.
[6] D. Akakoshi, Y. Ueda, J. Phys. Soc. Jpn. 68 (1999) 736.
[7] A. Maignan, C. Martin, D. Pelloquin, N. Nguyen, B. Raveau, J. Solid State Chem. 142 (1999) 247.
[8] C. Frontera, A. Caneiro, A.E. Carrillo, J. Oró-Solé, J.L. García-Muñoz, Chem. Mater. 17 (2005) 5439.
[9] M. Karppinen, M. Matvejeff, K. Salomäki, H. Yamauchi, J. Mater. Chem. 12 (2002) 1761.
[10] K. Conder, E. Pomjakushina, A. Soldatov, E. Mitberg, Mater. Res. Bull. 40 (2005) 257.
[11] J. Rodríguez-Carvajal, Physica B 192 (1993) 55.
[12] S. Streule, A. Podlesnyak, J. Mesot, M. Medarde, K. Conder, E. Pomjakushina, E. Mitberg, V. Kozhevnikov, J. Phys.: Condens. Matter 17 (2005) 3317.
[13] J.C. Burley, J.F. Mitchell, S. Short, D. Milelr, Y. Tang, J. Solid State Chem. 170 (2003) 339.
[14] P.S. Anderson, C.A. Kirk, J. Knudsen, I.M. Reaney, A.R. West, Solid State Sci. 7 (2005) 1149.
[15] Md.M. Seikh, V. Caignaert, V. Pralong, Ch. Simon, B. Raveau, J. Phys.: Condens. Matter 20 (2008) 015212.
[16] M. Respaud, C. Frontera, J.L. García-Muñoz, M.A.G. Aranda, B. Raquet, J.M. Broto, H. Rakoto, M. Goiran, A. Llobet, J. Rodríguez-Carvajal, Phys. Rev. B 64 (2001) 214401.
[17] V.P. Plakhty, Yu.P. Chernenkov, S.N. Barilo, A. Podlesnyak, E. Pomjakushina, E.V. Moskvin, S.V. Gavrilov, Phys. Rev. B 71 (2005) 214407.
[18] Y. Moritomo, T. Akimoto, M. Takeo, A. Machida, E. Nishibori, M. Takata, M. Sakata, K. Ohoyama, A. Nakamura, Phys. Rev. B 61 (2000) R13325.
[19] J.-E. Jørgensen, L. Keller, Phys. Rev. B 77 (2008) 024427.
[20] H.D. Zhou, J.B. Goodenough, J. Solid State Chem. 177 (2004) 3339.
[21] D.D. Khalyavin, D.N. Argyriou, U. Amann, A.A. Yaremchenko, V.V. Kharton, Phys. Rev. B 75 (2007) 134407.
[22] Yu.P. Chernenkov, V.P. Plakhty, V.I. Fedorov, S.N. Barilo, S.V. Shiryaev, G.L. Bychkov, Phys. Rev. B 71 (2005) 184105.
[23] In Ref. [20], it was shown that $YBaCo_2O_{5.5}$ consists of two phases with different unit cells. This was the case also with our R=Y sample. We have refined our data for the majority phase with the P-centered structure.
[24] C. Frontera, J.L. García-Muñoz, O. Castaño, C. Ritter, A. Caneiro, J. Phys.: Condens. Matter 20 (2008) 104228.
[25] D. Akahoshi, Y. Ueda, J. Solid State Chem. 156 (2001) 355.
[26] K. Conder, E. Pomjakushina, V. Pomjakushin, M. Stingaciu, S. Streule, A. Podlesnyak, J. Phys.: Condens. Matter 17 (2005) 5813.
[27] P. Karen, P.M. Woodward, P.N. Santhosh, T. Vogt, P.W. Stephens, S. Pagola, J. Solid State Chem. 167 (2002) 480;
P. Karen, J. Solid State Chem. 177 (2004) 281.
[28] G. Aurelio, J. Curiale, R.D. Sánchez, Physica B 384 (2006) 106.
[29] A. Podlesnyak, A. Karkin, K. Conder, E. Pomjakushina, M. Stingaciu, P. Allenspach, J. Magn. Magn. Mater. 316 (2007) E710.
[30] S. Roy, I.S. Dubenko, M. Khan, E.M. Condon, J. Craig, N. Ali, W. Liu, B.S. Mitchell, Phys. Rev. B 71 (2005) 024419.
[31] A.K. Kundu, B. Raveau, V. Caignaert, E.-L. Rautama, V. Pralong, J. Phys.: Condens. Matter 21 (2009) 056007.